Dalton Transactions

Accepted Manuscript

ROYAL SOCIETY OF CHEMISTRY

www.rsc.org/dalton

2-(2'-Hydroxyphenyl)-benzothiazole (HBT)-quinoline conjugate: Highly specific fluorescent probe for Hg^{2+} based on ESIPT and its application in bioimaging

Sunanda Sahana[a], Gargi Mishra[b], Sri Sivakumar[b], Parimal K. Bharadwaj[a]*
[a]Department of Chemistry, Indian Institute of Technology Kanpur, Kanpur-208016, India
[b]Department of Chemical Engineering, Indian Institute of Technology Kanpur, Kanpur-208016, India

A benzothiazole derived chemosensor **L** has been designed based on the excited state proton transfer (ESIPT) mechanism to afford a fluorescence turn-on response specifically in the presence of Hg^{2+} ion over a host of biologically relevant metal ions as well as toxic heavy metal ions. The chemosensor exhibits high sensitivity with the detection limit down to 0.11μM. The metal binding is supported by ^1H NMR titrations, ESI-MS spectral analysis and substantiated by theoretical calculations using the density functional theory. The probe shows cell membrane permeability and efficiency for the detection of Hg^{2+} in *HeLa* cells.

Introduction

The design and synthesis of Hg^{2+}-responsive fluorescence chemosensors have been receiving considerable attention due to various deleterious effects of the metal ion on human health and also on the environment.[1,2] Toxicity of elemental or ionic forms of mercury arises due its high affinity for thiol groups in proteins and enzymes leading to dysfunction of cells[3-5] and consequently causing a wide variety of diseases such as prenatal brain damage, serious cognitive and motion disorders,[6] Minamata disease[7,8] and so on. High concentration of inorganic mercury contamination can arise from both natural sources like volcanic emissions[9] and anthropogenic sources like gold and coal mining,[10] solid waste interaction, combustion of fossil fuels etc.[11,12] In

the atmosphere, mercury vapors are eventually oxidized to Hg^{2+} and ultimately accumulates in fresh water and marine ecosystems where some microorganisms like prokaryotes and bacteria convert inorganic mercury into methylmercury. Because of its lipophilic nature, methylmercury can enter the food chain and bio-accumulates in higher organisms leading to diseases.[13] In drinking water United State Enviromental Protection agency standards allows maximum limit of Hg^{2+} to be 2 ppb.[14] Therefore, new mercury detection methods those are sensitive, cost effective, rapid, facile and non-hazardous to environment besides being suitable for biological applications are highly desirable.

In recent years many analytical detection methods such as atomic absorption spectroscopy, an inductively coupled plasma-mass spectrometry and inductively coupled plasma-atomic emission spectrometry have been developed.[15,16] Among these, the fluorescence chemosensing technique is more sought after and is being explored due to its high sensitivity, real-time detection, low detection limit, portability and operational simplicity.

For the optical detection of various analyte, the UV-visible absorption and fluorescence spectral changes can be originated from different mechanisms.[17] Especially, fluorescence sensing based on excited-state intramolecular proton transfer (ESIPT) is quite promising by virtue of its large Stokes shift, good photo-stability, intramolecular hydrogen-bonded property, and spectral sensitivity to the surrounding medium.[18-20] The molecules capable of ESIPT usually exist exclusively in the energetically favorable enol (E) form in the ground state and as keto form in the excited state. Upon excitation an extremely fast migration of a proton takes place between the two complementary centers via intramolecular hydrogen bond in the first excited state. The molecule 2-(2'-hydroxyphenyl)-benzothiazole (HBT) is a potentially interesting moiety as an ESIPT fluorophore.[21-30]

Herein, we report the synthesis of the probe **L** where 5-(benzothiazol-2-yl)-4-hydroxyisophthalaldehyde is covalently attached with 8-aminoquinoline by Schiff base condensation as the exclusive product. In this design, the 8-aminoquinoline moiety can facilitate a metal ion to anchor near the phenol moiety so that the ESIPT process can be disrupted. In fact, we find this probe possesses high selectivity, sensitivity, reversibility and operation under physiological pH. These properties make it suitable for fluorescence imaging of Hg^{2+} in *HeLa* cells and making it possible for in situ detection at a low concentration in acetonitrile: water medium.

Experimental

Materials and methods

Reagent grade 8-aminoquinoline and all metal perchlorate salts were acquired from Aldrich Chemicals (USA) and were used as received. Salicylaldehyde, 2-aminothiophenol, hexamine, trifluoroacetic acid, sodium borohydride and the solvents were procured from S. D. Fine Chemicals (India). All the solvents were purified prior to use following standard procedures. Chromatographic separations were done by column chromatography using neutral alumina or silica gel (100-200 mesh) from S. D. Fine Chemicals (India). The variation of pH was achieved with dilute HCl and NaOH.

All the synthesized compounds were characterized by different spectroscopic methods. Both ^{1}H NMR (500 MHz) and ^{13}C NMR spectra (125 MHz) of the compounds were recorded on a JEOL DELTA2 spectrometer in $CDCl_3$ and DMSO-d_6 with TMS as the internal standard. The ESI-MS data were obtained from a WATERS Q-Tof Premier Mass Spectrometer. UV-vis spectra were recorded on a Shimadzu 2450 UV-vis spectrophotometer in MeCN:H_2O (3:2, v/v, 10 mM HEPES buffer, pH = 7) at 21 °C. Fluorescence emission spectra were obtained on a Perkin-

Elmer LS 50B Luminescence Spectrometer at 21 °C. The imaging system was Olympus Ix81 motorized inverted fluorescence microscope. The pH of different solutions were measured by using a pH meter model Eco testr pH I by Thermo Scientific (USA).

UV-vis and fluorescence spectroscopic studies

Luminescence properties of **L** were checked in mixed solvent MeCN: H_2O (3:2, v/v, 10 mM HEPES buffer, pH = 7). Stock solution of **L** was prepared as 10^{-3} M in 25 mL of MeCN and then diluted to the desired concentration. Stock solutions of various ions were prepared at the concentration of ~10^{-3} M in 25 mL distilled water and then diluted to the desired concentrations. Absorbance and fluorescence spectral data were recorded 10 min after the addition of the ions. For fluorescence measurements, excitation wavelength was 340 nm (slit width = 10/10 nm) and emission was acquired from 360 nm to 675 nm.

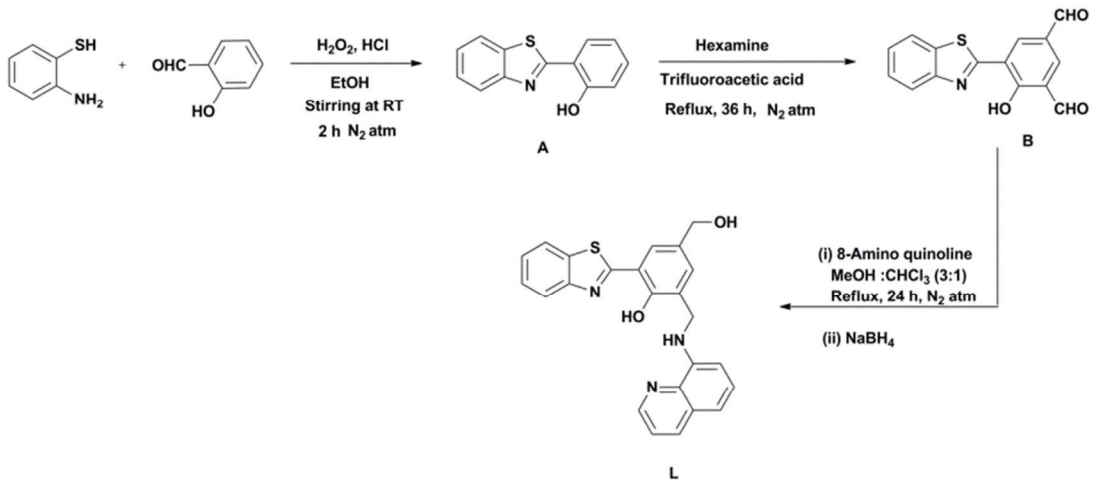

Scheme 1: Synthesis of the chemosensor, **L**

Synthesis of the chemosensor

The probe **L** was synthesized in several steps as illustrated in Scheme 1 where **A** is 2-(2'-Hydroxyphenyl)-benzothiazole and **B** is 5-(benzothiazol-2-yl)-4-hydroxyisophthalaldehyde.

Synthesis of A [2-(2'-Hydroxyphenyl)-benzothiazole]

Compound **A** was synthesized following a reported method.[31] A 30 mL ethanolic solution of salicylaldehyde (2.51g, 20.6 mmol) and 2-aminothiophenol (2.34 g, 18.7 mmol) was allowed to stir for 30 min at RT and then treated with hydrogen peroxide (30%) (2.31 mL, 74.8 mmol) and hydrochloric acid (37.5%) (1.14 mL, 37.3 mmol) under N_2 atmosphere. Stirring continued at RT for another 2 h. The reaction mixture was then poured into crushed ice and then extracted with ethyl acetate (EtOAc). The organic layer was dried over anhydrous sodium sulphate. The crude product was purified by column chromatography (silica gel, 100 -200 mesh, EtOAc: hexane = 5:95, v/v) as a white crystalline solid (2.9 g, 68% yield).m.p. 134 °C; ^{1}H NMR (500 MHz, DMSO- d_6 25 °C, $Si(CH_3)_4$) δ: 11.55 (s, 1H), 8.15(d, 1H, J = 7.95Hz), 8.11 (d, 1H, J = 7.95 Hz), 8.03(d, 1H, J = 8.25 Hz), 7.52(t, 1H, J = 7 Hz), 7.43- 7.36 (m,2H), 7.00 (t, 1H J = 7.95 Hz), 6.98 (t, 1H, J = 7.95Hz) (Fig. S1); ^{13}C NMR (125 MHz, $CDCl_3$, 25 °C, $Si(CH_3)_4$) δ: 116.87, 117.96, 119.61, 121.61, 122.27, 125.64, 126.79, 128.51, 132.67, 132.85, 151.92, 158.03, 169.47. (Fig. S2). ESI MS: (m/z): Calculated for 228.05 $[M + H^+]^+$ Found 228.04 (Fig. S3). Elemental analysis: calculated (%) for $C_{13}H_9NO$: C 68.69, H 3.99, N 6.16; found: C 68.56., H 4.07, N 6.19.

Synthesis of B [5-(benzothiazol-2-yl)-4-hydroxyisophthalaldehyde]

In a 250 mL round bottom flask, compound **A** (0.5 g, 2.19 mmol) was dissolved in 50 mL trifluoroacetic acid and the solution was cooled in an ice-bath. It was followed by an addition of hexamine (1.8 g, 12.85 mmol) in small amount at a time over a period of 30 min. The resulting solution was heated to 145 °C for 36 h under N_2 atmosphere till it turned dark brown. The hot solution was allowed to cool to RT and poured into100 mL 4N HCl solution and finally extracted with ethyl acetate (EtOAc). After drying the organic layer over anhydrous sodium sulphate, the

solvent was completely removed to afford a yellow solid. The crude product was purified by column chromatography (silica gel, 100 -200 mesh, EtOAc: hexane = 15:85, v/v) as a yellow crystalline solid (150 mg, 24% yield).^{1}H NMR (500 MHz, DMSO-d_6): 10.36 (s, 1H), 10.00 (s, 1H), 8.84 (s, 1H), 8.36 (s, 1H), 8.21 (d, 1H, J = 7.6 Hz), 8.14 (d, 1H, J = 8.85 Hz), 7.57 (t, 1H J = 7.6 Hz), 7.50 (t, 1H J = 7.65 Hz). (Fig. S4). ^{13}C NMR (125 MHz, DMSO-d_6, 25 °C, $Si(CH_3)_4$) δ: 31.24, 122.89, 122.97,124.54,126.54,127.64, 134.19, 134.36, 135.59, 164.74, 191.44, 191.89, ,(Fig. S5). ESI MS: (m/z): $[M + H^+]^+$ Calculated for 284.04 Found 284.03(Fig. S6). Elemental analysis: calculated (%) for $C_{15}H_9NO_3S$: C 63.59, H 3.20, N 4.94; found: C 63.75, H 3.16, N 4.67.

Synthesis of L

To a solution of compound **B** (0.25 g, 0.8 mmol) in 45 mL dry methanol, 8-aminoquinoline (0.278 g, 1.9 mmole) was added and refluxed for 24 h under N_2 atmosphere. A red precipitate settled at the bottom which was collected by filtration and reduced by excess sodium borohydride in methanol by stirring at room temperature for 6 h. Upon solvent removal, the residue was dissolved in dichloromethane and washed with brine. The organic layer was dried over anhydrous sodium sulphate. Purification of **L** was achieved by column chromatography (neutral alumina, EtOAc: hexane = 10: 90, v/v) as a light yellow solid (225 mg, 61% yield). ^{1}H NMR (500 MHz,$CDCl_3$,25 °C, $Si(CH_3)_4$ δ: 12.97 (s, 1H), 8.73(s, 1H), 8.06 (d, 1H J = 6.1Hz), 7.97(d, 1H J = 7.65Hz), 7.90(d, 1H J = 7.65Hz), 7.62 (s, 1H), 7.49 (t, 1H, J = 7.65Hz), 7.45 (s, 1H), 7.42 (d, 1H, J = 7.65 Hz), 7.37 (t, 1H, J = 4.6 Hz), 7.32 (t, 1H, J = 7.65 Hz), 7.05 (d, 1H, J = 7.65 Hz), 6.69 (d, 2H, J = 7.65 Hz), 4.7 (d, 2H, J= 6.15 Hz), 4.59 (s, 2H) (Fig. S7) ^{13}C NMR (125 MHz, $CDCl_3$, 25 °C, $Si(CH_3)_4$) δ: 31.02, 42.45, 64.84, 105.26, 114.22, 116.37, 121.37, 121.48, 121.66, 122.19, 125.68, 126.02, 126.83, 127.89, 128.76, 130.55, 131.89, 132.75, 136.14,

138.40, 144.65, 147.04, 151.79, 155.55, 169.42,(Fig. 8).ESI MS: (m/z): $[M + H^+]^+$ Calculated for 414.13 Found 414.1267 (Fig. S9). Elemental analysis: calculated (%) for $C_{24}H_{19}N_3O_2S$: C 69.79, H 4.64, N 10.17; found: C 69.65, H 4.56, N 10.26. In spite of repeated attempts the dialdehyde **B** did not afford any diimine product even when large excess of 8- aminoquinoline was used. This may be due to steric reasons which we did not probe any further.

Cell imaging

To establish *in vitro* chemosensing abilities of **L**, it was checked for its cellular uptake and its binding with mercury salt exposed mammalian cells. For this purpose, *HeLa* cells were cultured in DMEM medium containing penicillin/streptomycin (1% v/v) and FBS (10% v/v) in 5% CO_2 at 37 °C. 10^4 cells were added in each well of the 24 welled tissue culture plates and incubated for 6h in a CO_2 incubator. After 6 h, *HeLa* cells were incubated with mercury perchlorate salt (30 μM) dispersed in HEPES buffer (10 mM) which was added to the cell culture media. After 18 h, the media was removed from the plate and fresh media with **L** (10 μM) was added and incubated for 1 h. After 1h, cells were washed with PBS, and fixed with 4% formaldehyde solution for 20 min. The nuclei of the cells were stained with Hoescht stain for 10 min followed by washing with PBS. The nucleus was also stained with 10μg/ml Hoechst dye and imaged with optical fluorescence. The staining protocols were used as provided by the suppliers. The cells were again washed with PBS and observed under fluorescence microscope to monitor the metal salt-**L** binding inside the cells using Olympus Ix81 motorized inverted fluorescence microscope. Cells without Hg^{2+} salt treatment but incubated with ligand were used as the negative control. The images of the cell were recorded by fluorescence microscopy at 540 nm (λ_{ex}= 340nm).

Results and discussion

Photophysical properties

Metal-free **L** exhibits several absorption bands in the region 260-360 nm. The absorption band (Fig. 1a) at 266 nm is reminiscent of the 8-aminiqinoline moiety[32] while the bands at 300 nm and 355 nm are due to the benzothiazole group[33,34] present in the dye. On gradual addition of Hg^{2+} to the solution of **L** the 266 nm band decreases in intensity with a blue-shift to ~250 nm. The 300 nm band, on the other hand, makes a slight red-shift appearing as a shoulder at 355 nm. This band also increases in intensity quite significantly. Addition of Hg^{2+} also results in color change of the solution from colorless to yellow within 10 min. In presence of Fe^{3+} or Cr^{3+} ion, similar behavior is observed albeit to a lesser degree. In contrast, alkali/alkaline earth, transition and Cd^{2+}, Al^{3+}, Ag^{+}, and Pb^{2+} metal ions do not show any changes in the UV-vis spectra.

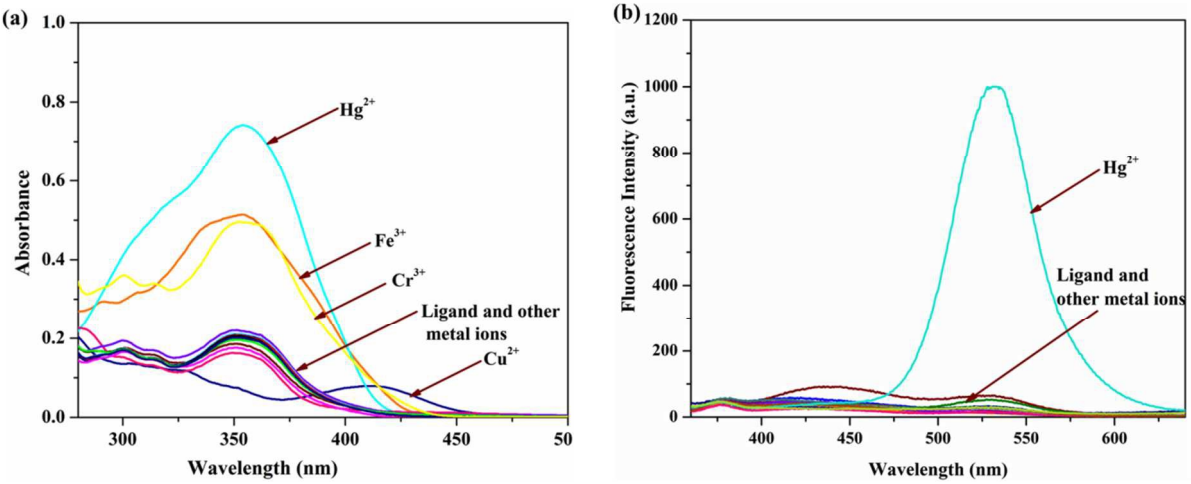

Fig. 1 (a) Absorbance spectra of **L** (10 μM) in MeCN: H_2O (3:2, v/v, 10 mM HEPES Buffer, pH = 7) in the presence of 10 equivalent of various metal ions. (b) Fluorescence spectra of **L** (10 μM) in MeCN: H_2O (3:2, v/v, 10 mM HEPES Buffer, pH = 7) in the presence of 10 equivalent of various metal ions. λ_{ex} = 340 nm ; Slit = 10 /10 nm

Upon excitation at 340 nm, metal-free **L** shows emission with very low intensity at 377 nm (Φ = 0.007) due to the ESIPT being operational which is the major deactivation pathway.

However, upon addition of 10 equivalent of Hg^{2+} ion, it engages the phenolate oxygen (O) atom preventing ESIPT with the result of a strong emission ($\Phi = 0.527$) band centering at 530 nm (Fig. 1b). Addition of any other metal ion (*vide supra*) does not elicit any emission that is noticeably different from that of the metal-free **L**.

In order to evaluate the practical applicability of **L** as a chemosensor for the Hg^{2+} ion, it was further subjected to competitive experiments by adding 10. equivalent of Hg^{2+} to the **L** solution in the presence of 100 equivalent of another metal ion from the list: Na^{+}, K^{+}, Ca^{2+}, Mg^{2+}, Mn^{2+}, Fe^{2+} Co^{2+}, Ni^{2+}, Cu^{2+}, Zn^{2+},Cd^{2+}, Ag^{+}, Pb^{2+}, Cr^{3+}, Al^{3+} and Fe^{3+} under identical condition. A look at the Fig. 2 shows almost no interference of any of these metal ions on the sensing of Hg^{2+}.

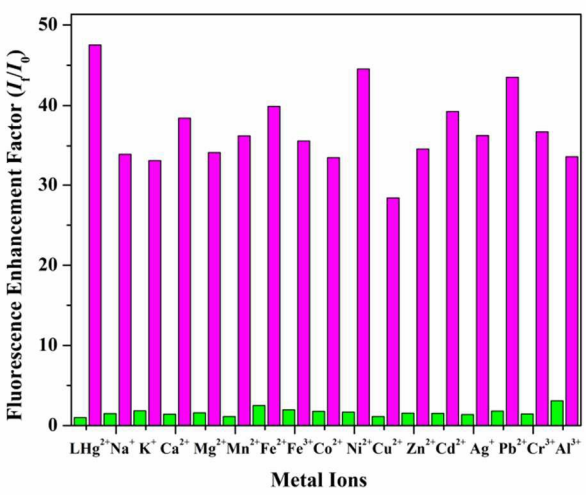

Fig. 2 Selectivity of the dye **L** (10 μM) for the Hg^{2+} ion in MeCN: H_2O (3:2, v/v, 10 mM HEPES Buffer, pH = 7). Green bars indicate the emission responses of the dye with 100 equivalent of the metal ions of interest, and pink bars represent the final integrated fluorescence response after the addition of 10 equivalent of $Hg^{2+}$to each solution containing other metal ions. λ_{ex}= 340 nm; Slit = 10/10 nm.

Job's plot obtained from emission data indicates a binding stoichiometry of 1:1 for ligand to Hg^{2+} (Fig. S12). The association constant for Hg^{2+} was estimated to be 1.24×10^4 M^{-1} on the

basis of linear fitting of the fluorescence titration (Fig. 3a**)** curve assuming 1:1 stoichiometry using Benesi−Hildebrand plot (Fig.3b).[13] Besides, in mass spectrum a peak at m/z 691.4230 assigned to $[L\text{-}H+Hg^{2+}+2H_2O+MeCN]^+$ (Fig. S10) also supports 1:1 binding stoichiometry.

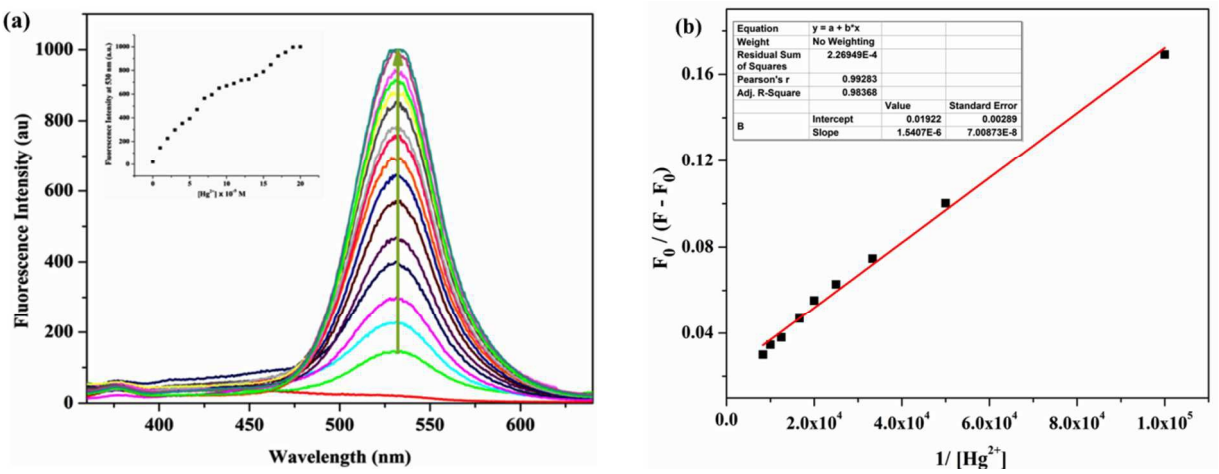

Fig. 3 (a) Fluorescence titration of **L** with increasing Hg^{2+} ion concentration in 3:2 MeCN: H_2O (HEPES Buffer 10mM, pH = 7). λ_{ex} = 340 nm. Arrow indicates the increasing trend in Hg^{2+} ion concentration. (b) Binding constant plot of **L** for Hg^{2+}

Based on the fluorescence titration data, the detection limit of **L** to Hg^{2+} was calculated to be 0.11 μM by plotting emission intensity at 530 nm against concentration of Hg^{2+} (Fig S13). .These results clearly demonstrate that the probe is highly efficient to monitor Hg^{2+} levels both qualitatively and quantitatively.

The reversibility behavior of **L** – Hg^{2+} complex was also studied. In presence of 10 equivalent of Na_2S, the emission of the complex is totally quenched within 10 minutes (Fig.4) due to removal of the Hg^{2+} ion by S^{2-} with concomitant formation of the free ligand and HgS. Thus, **L** behaves as a highly selective reversible fluorescence "ON" chemosensor for the Hg^{2+} ion in presence of various cations and anions except S^{2-}.

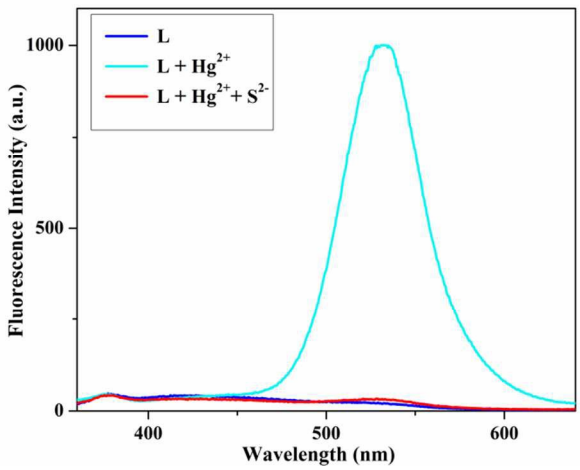

Fig.4 Reversible behavior of **L** and its Hg^{2+} complex in mixed MeCN: H_2O (3:2, v/v, 10 mM HEPES Buffer, pH = 7). λ_{ex} = 340 nm ; Slit = 10 /10 nm.

For its possible application in biology, the effects of pH on the fluorescence response of **L** and **L**-Hg^{2+} systems have also been studied. The dye is found to be almost pH insensitive and stable in the pH range, 5-9. Below pH 4, moderate fluorescence intensity is observed for **L** due to protonation of benzothiazole N and OH atoms preventing the ESIPT process. After the addition of 10 equivalent of Hg^{2+}, the fluorescence intensity remains almost same in the pH~4, but a sharp increase in fluorescence intensity is observed in the pH range of 5-8 compared to **L** (Fig 5). A further increase in the pH causes the fluorescence intensity to decrease. So, **L** displays the best response for Hg^{2+} in the pH region 5-8.

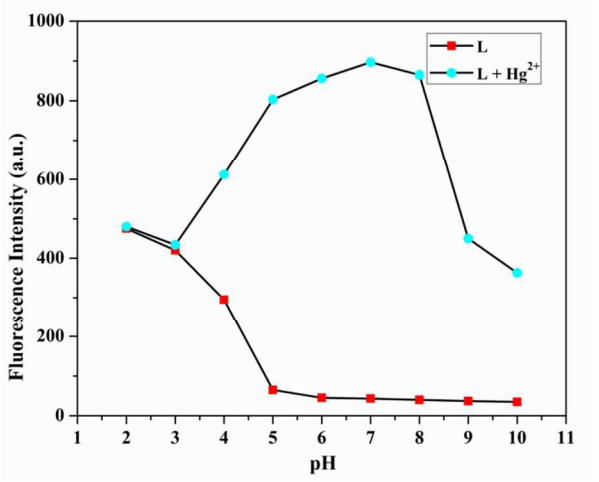

Fig. 5 The fluorescence intensity changes at 530 nm of **L** and **L**-Hg^{2+} solution at various pH conditions. λ_{ex} = 340 nm; Slit = 10 /10 nm.

^{1}H NMR titration

To ascertain the possible binding site for the Hg^{2+} ion, ^{1}H NMR titration experiment was carried out in $CDCl_3$ (Fig. 6). Upon addition of Hg^{2+} ion to the solution of **L**, the proton signal at 12.9754 ppm disappeared suggesting binding of the phenolate O atom to Hg^{2+}. The proton H_b adjacent to the nitrogen of the phenyl ring of 8-aminoquinoline exhibits a downfield shift (from 8.0630 ppm to 8.2132 ppm) clearly indicating this N atom to be involved in the metal binding. In addition, the down-field shift (from 8.7325 ppm to 8.8086 ppm) for H_c proton of the quinoline moiety indicates the involvement of NH unit in the complexation. Thus, the proposed binding of **L** with Hg^{2+}occurs through the phenolate O atom of benzthiazole unit and the two N atoms of 8-aminoquinoline moiety in a tridentate fashion. The other coordination sites on the metal ion might be occupied by solvent molecules.

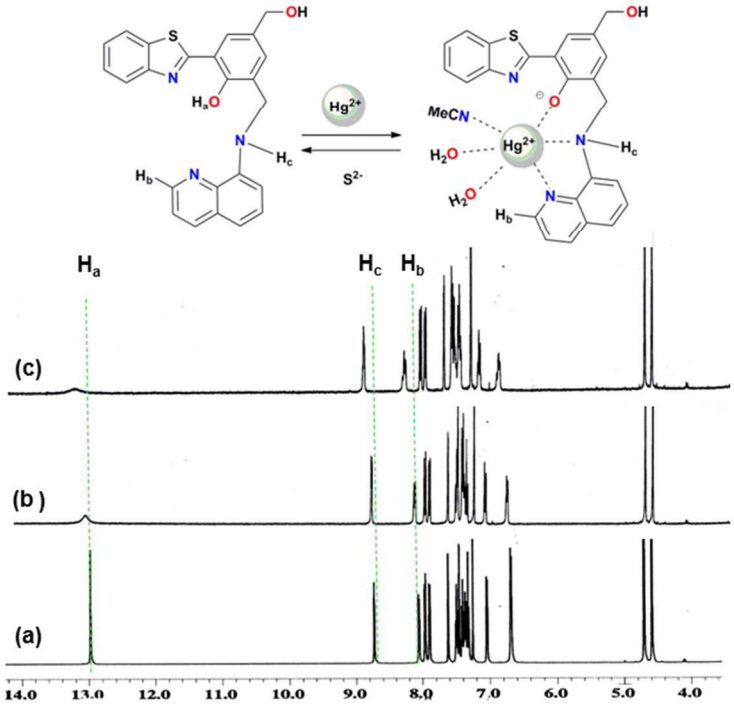

Fig. 6 Proposed binding mode of **L** with Hg^{2+}.(a) **L** only, (b) **L** and 0.5 equivalent of Hg^{2+}, (c) **L** and 1 equivalent of Hg^{2+}

Density functional theory (DFT) calculations

To explain the ESIPT process DFT calculation were performed using the Gaussian 09 programme.[35] The keto and enol forms of **L** were optimized with the B3LYP[36-41] functional and 6-311+G (d,p) basis set. For Hg^{2+} bound species, LANL2DZ for Hg and 6-31g*+ for the rest of the atoms were used for optimization. The optimized structures of **L** and its complex with Hg^{2+} are shown in Figure 7. As can be seen in Fig. 7 the distance between the H of hydroxyl and N in enol form is 1.731Å, satisfying the excited state intramolecular proton transfer (ESIPT) requirements.

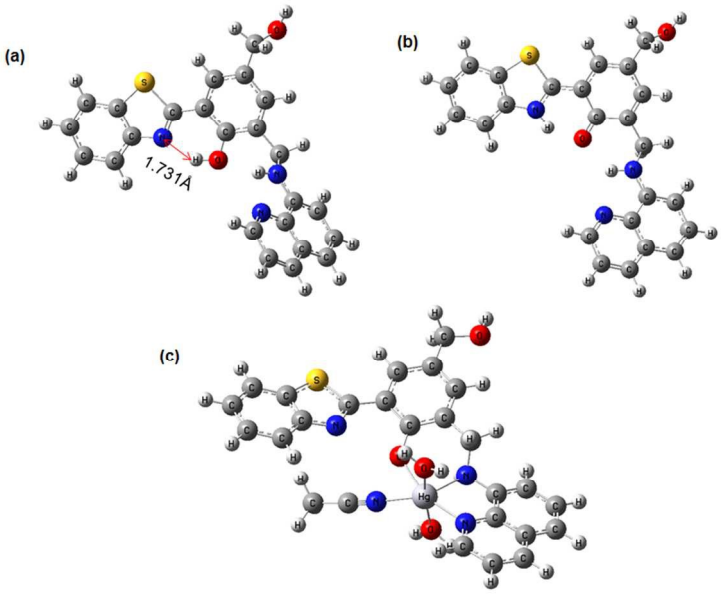

Fig.7 Optimized structures of (a) enol form of **L** (b) keto form of **L** (c) **L**-Hg^{2+} complex

Cell imaging

To analyze the biological fluorimetric detection potential of **L**, cell imaging based detection analysis was done on *HeLa* cells. Cells were incubated with mercury perchlorate (30 μM) to allow the internalization of the salt inside the cells. Mercury perchlorate exposed cells were then fluorometrically detected by addition of **L**. The complexation of **L** and mercury perchlorate gives strong green fluorescence (λ_{max} = 530 nm). The accumulation of mercury ions inside the cells was visualized by binding of mercury salts with **L** (Fig 8). The green fluorescence accumulated inside the cells indicate the presence of mercury salts inside the cells detected by **L**. This fluorescence microscopic analysis strongly suggests that our synthesized chemosensor is cell membrane permeable and recognizes intracellular Hg^{2+}.

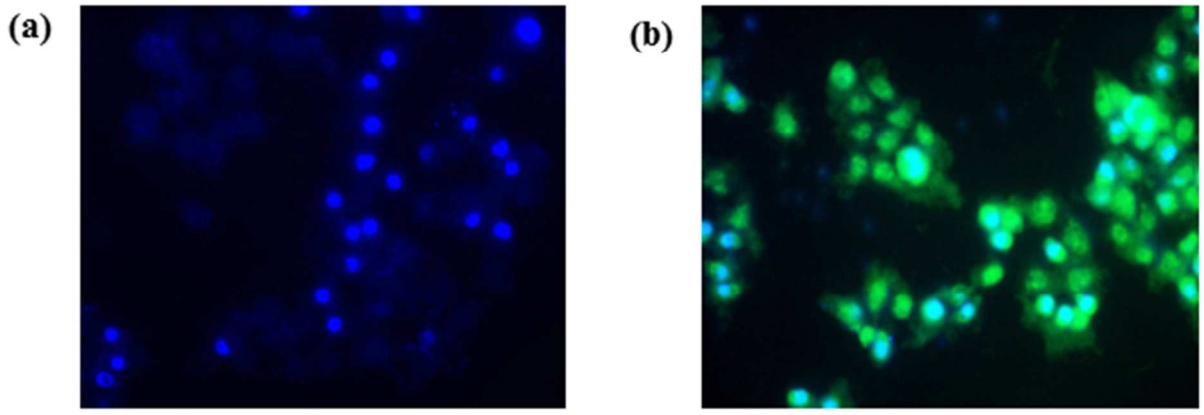

Fig.8 Fluorescence images of *HeLa* cells. (a) fluorescence image of *HeLa* cells incubated with **L** (10 μM) for 1 h. (b) fluorescence image of *HeLa* cells first incubated with mercury perchlorate (30 μM) for 1 h. and then after adding **L** (10 μM) for 30 min

Conclusion

In summary, we have demonstrated a molecular fluorescence sensor for Hg^{2+} based on metal induced inhibition of ESIPT mechanism. In view of the high selectivity, sensitivity, **L** is potentially useful as Hg^{2+} sensor in MeCN: H_2O (3:2, v/v, 10 mM HEPES Buffer) medium at a wide pH range. The detection limit of the **L** with Hg^{2+} is 0.11μM which shows its good

sensitivity. A comparison study for recent ESIPT based chemosensors for Hg^{2+} is also shown (Table 1 in ESI). The possible binding modes between the **L** with the Hg^{2+} ion are investigated by the Job' plot, ESI-MS and ^{1}H NMR titration experiments. Moreover, the sensor is also applicable for the detection of Hg^{2+} in *HeLa* cells as shown by the fluorescence microscopic images.

Acknowledgements

This work was supported by Department of Science and Technology, New Delhi, India (No. SERB/CHM/20130239 to P.K.B). S.S. thanks Council of Scientific and Industrial Research (CSIR) India for senior research fellowship. For cell imaging study the department of Chemical Engineering, Indian Institute of Technology is gratefully acknowledged. For Gaussian calculation HPC 2010 facility of IIT Kanpur is gratefully acknowledged.

References

1. E. M. Nolan and S. J. Lippard, *Chem. Rev.*, 2008, **108**, 3443-3480.

2. G. -B. Jiang, J. -B. Shi and X. - B. Feng, *Environ. Sci. Technol*., 2006, **40**, 3672-3678.

3. P. Grandjean, P. Weihe, R. F. White and F. Debes, *Environ. Res*., 1998, **77**, 165-172.

4. T. Takeuchi, N. Morikawa, H. Matsumoto and Y. Shiraishi, *Acta Neuropathol*., 1962, **2**, 40-57.

5. M. Harada, *Crit. Rev. Toxicol*., 1995, **25**, 1-24.

6**.** P. W. Davidson, G. J. Myers, C. Cox, C. F. Shamlaye, D. O. Marsh, M. A. Tanner, M. Berlin, J. Sloane-Reeves, E. Cernichiari, O. Choisy, A. Choi and T.W. Clarkson, *Neurotoxicol*., 1995, **16**, 677-688.

7. G. E. Mckeown-Eyssen, J. Ruedy and A. Neims, *Am. J. Epidemiol*., 1983, **118**, 470-479.

8. Z. Zhang, D. Wu, X. Guo, X. Qian, Z. Lu, Q. Zu, Y. Yang, L. Duan, Y. He and Z. Feng, *Chem. Res. Toxicol.*, 2005, **18**, 1814-1820.

9. A. Renzoni, F. Zino and E. Franchi*, Environ. Res*., 1998, **77**, 68-72.

10. K. Rurack, M. Kollmannsberger, U. Resch-Genger and J. Daub, *J. Am.Chem. Soc*., 2000, **122**, 968-969.

11. J. M. Benoit, W. F. Fitzgerald and A. W. Damman, *Environ. Res.*, 1998, **78**, 118-133.

12. O. Malm, *Environ. Res*., 1998, **77,** 73-78.

13. P. Chu, D. B. Porcella, *Water, Air, Soil Pollut*. 1995, **80**, 135-144.

14. Mercury Update: Impact on Fish Advisories; EPA Fact Sheet EPA- 823-F-01-001; Environmental Protection Agency, Office of Water: Washington, DC, 2001.

15. W. J. McShane, R. S. Pappas, V. Wilson-McElprang and D. Paschal, *Spectrochim. Acta, Part B*, 2008, **63**, 638-644.

16. M. de la Guardia, A. R. Mauri and C. J. Mongay, *J. Anal. At. Spectrom.,* 1988, **3**, 1035-1038.

17. J. Wu, W. Liu, J. Ge, H. Zhang and P. Wang, *Chem. Soc. Rev.,* 2011, **40**, 3483-3495.

18. Z. Liu, W. He, and Z. Guo, *J. Chem. Soc. Rev*., 2013, **42**, 1568-1600.

19. P. Majumder and J. Zhao, *J. Phys. Chem. B.,* 2015, **119**, 2384-2394.

20. J. Zhao, S. Ji, Y. Chen, H. Guo and P. Yang, *Phys. Chem. Chem. Phys.,* 2012, **14,** 8803-8817.

21. T. -I. Kim, H. J. Kang, G. Han, S. J. Chung and Y. Kim, *Chem. Commun*., 2009, **45,** 5895-5897.

22. R. Hu, J. Feng, D. Hu, S. Wang, S. Li, Y. Li and G. Yang, *Angew. Chem. Int. Ed.,* 2010, **49**, 4915-4918.

23. L. Wang, Q. Zang, W. Chen, Y. Hao, Y.-N. Liu and J. Li, *RSC Adv.,* 2013, **3**, 8674-8676.

24. S. Liu, L. Zhang, W. Zan, X. Yao, Y. Yang and X. Liu, *Sens. Actuators. B.*, 2014, **192**, 386-392.

25. Z. Xu, L. Xu, J. Zhou, Y. Xu, W. Zhu and X. Qian, Chem. Commun., 2012, **48**, 10871-10873.

26. S. Goswami, A. Manna, S. Paul, A. K. Das, P. K. Nandi, A. K. Maity, and P. Saha, *Tetrahedron Lett*., 2014, **55**, 490-494.

27. S. Goswami, A. Manna, M. Mondal and D. Sarkar, *RSC Adv*., 2014, **4**, 62639-62643.

28. T. Raj, P. Saluja, N. Singh, and D.O. Jang, *RSC Adv.,*2014, **4**, 5316-5321.

29. J. Wang, X. Liu and Y. Pang, *J. Mater. Chem. B,* 2014, **2**, 6634-6638.

30. S. Goswami, S. Maity, A. C. Maity, A. K. Das, B. Pakhira, K. Khanra, N. Bhattacharyya and S. Sarkar*, RSC Adv.,* 2015, **5**, 5735-5740.

31. S. Goswami, A. Manna, S. Paul, A. K. Das, K. Aich and P. K. Nandi, *Chem. Commun.,* 2013, **49**, 2912-2914.

32. E. A. Steck, G. W. Ewing, F. Nachod, *J. Am. Chem. Soc*., 1948, **70**, 3397-3406.

33. T. Elsaesser, B. Schmetzer, M. Lipp and R. J. Bauerle, *Chem.Phys.Lett.,* 1988, **148**, 112-118.

34. O. F. Mohammed, S. Luber, V. S. Batista, and E. T. J. Nibbering, *J. Phys. Chem. A*., 2011, **115**, 7550-7558.

35. M. J. Frisch, G. W. Trucks, H. B. Schlegel, G. E. Scuseria, M. A. Robb, J. R. Cheeseman, G. Scalmani, V. Barone, B. Mennucci, G. A. Petersson, H. Nakatsuji, M. Caricato, X. Li, H. P. Hratchian, A. F. Izmaylov, J. Bloino, G. Zheng, J. L. Sonnenberg, M. Hada, M. Ehara, K. Toyota, R. Fukuda, J. Hasegawa, M. Ishida, T. Nakajima, Y. Honda, O. Kitao, H. Nakai, T. Vreven, J. A. Montgomery, Jr., J. E. Peralta, F. Ogliaro, M. Bearpark, J. J. Heyd, E. Brothers, K. N. Kudin, V. N. Staroverov, T. Keith, R. Kobayashi, J. Normand, K. Raghavachari, A. Rendell,

J. C. Burant, S. S. Iyengar, J. Tomasi, M. Cossi, N. Rega, J. M. Millam, M. Klene, J. E. Knox, J. B. Cross, V. Bakken, C. Adamo, J. Jaramillo, R. Gomperts, R. E. Stratmann, O. Yazyev, A. J. Austin, R. Cammi, C. Pomelli, J. W. Ochterski, R. L. Martin, K. Morokuma, V. G. Zakrzewski, G. A. Voth, P. Salvador, J. J. Dannenberg, S. Dapprich, A. D. Daniels, O. Farkas, J. B. Foresman, J. V. Ortiz, J. Cioslowski and D. J. Fox, *Gaussian 09, Revision D.01,* Gaussian, Inc., Wallingford, CT, 2013.

36. A. D. Becke, *J. Chem. Phys*., 1993, **98**, 5648-5652.

37. C. Lee, W. Yang and R. G. Parr, *Phys. Rev. B. Condens. Matter.,* 1988, **37,** 785-789.

38. D. Andrae, U. Haeussermann, M. Dolg, H. Stoll and H. Preuss, *Theor. Chim. Acta.*, 1990, **77**, 123-141.

39. M. Cossi, N. Rega, G. Scalmani, V. Barone*, J. Comput. Chem.,* 2003, **24**, 669-681.

40. M. Cossi, V. Barone, *J. Chem. Phys.,* 2001, **115,** 4708-4717.

41. V. Barone, M. Cossi, *J. Phys. Chem. A.,* 1998, **102,** 1995-2001.

Graphical Abstract

2-(2'-Hydroxyphenyl)-benzothiazole (HBT)-quinoline conjugate: Highly specific fluorescent probe for Hg^{2+} based on ESIPT and its application in bioimaging

Sunanda Sahana[a], Gargi Mishra[b], Sri Sivakumar[b], Parimal K. Bharadwaj[a]*

[a]Department of Chemistry, Indian Institute of Technology Kanpur, Kanpur-208016, India

[b]Department of Chemical Engineering, Indian Institute of Technology Kanpur, Kanpur-208016, India

A new benzothiazole-based 8-aminoquinoline functionalized compound as a selective and sensitive fluorogenic chemosensor for Hg^{2+} and also being used in cell imaging.